Applied Catalysis B: Environmental 164 (2015) 316–323

Contents lists available at ScienceDirect

Applied Catalysis B: Environmental

journal homepage: www.elsevier.com/locate/apcatb

Preparation of Ni–Mg/β-SiC catalysts for the methane tri-reforming: Effect of the order of metal impregnation

Jesús Manuel García-Vargas*, José Luís Valverde, Javier Díez, Paula Sánchez, Fernando Dorado

Departamento de Ingeniería Química, Facultad de Ciencias Químicas, Universidad de Castilla-La Mancha, Avenida Camilo José Cela 12, 13005 Ciudad Real, Spain

ARTICLE INFO

Article history:
Received 24 July 2014
Received in revised form
16 September 2014
Accepted 20 September 2014
Available online 6 October 2014

Keywords:
Methane
Tri-reforming
Nickel
Magnesium
TPO

ABSTRACT

The influence of the order of Ni and Mg impregnation has been analyzed in terms of catalytic activity and stability of β-SiC supported catalysts for the tri-reforming of methane. Catalysts were characterized using different techniques such as Temperature Programmed Reduction, X-Ray Diffraction, Transmission Electron Microscopy and Temperature Programmed Oxidation. The addition of Mg clearly changed the reduction profile, increasing the temperature required to obtain Ni^0. Higher reduction temperatures were needed when Mg was firstly loaded or when both metals, Ni and Mg, were simultaneously loaded, which was attributed to the occurrence of interactions between Ni and Mg. Catalyst prepared by first Ni impregnation showed the worst catalytic behaviours, probably due to a poor interaction between Ni and Mg, a possible blockage of Ni particles by Mg ones and the occurrence of Ni_2Si after reaction. Catalysts prepared with the highest Mg/Ni molar ratio (1/1) showed smaller Ni particle sizes, lower coke rate formation and higher basicity and Ni-Mg interaction. Ni-Mg/SiC 1/1 was selected as the best catalyst due to its high catalytic activity and stability and low coke generation.

© 2014 Elsevier B.V. All rights reserved.

1. Introduction

Nowadays, global warming is one of the most important environmental problems, usually related to the emission of green house gases like CH_4 and CO_2, and the raise observed in the atmospheric CO_2 concentration during the last century, which is assigned to human activities and the burning of fossil fuels. Therefore, CO_2 conversion and utilization are important elements in chemical research on sustainable development, but its recovery from concentrated sources requires substantial energy input [1], which makes interesting its conversion without previous separation.

Tri-reforming is an interesting process from an environmental point of view as it can help to reduce emissions of two green house effect gases like CH_4 and CO_2. In addition, this process enables the production of synthesis gas from a renewable source like biogas. Biogas is a clean and environmentally friendly fuel that is typically generated from anaerobic degradation of biomass. Biogas, consisting mainly of CO_2 and CH_4, is an attractive renewable carbon source and its exploitation would be advantageous from both financial and environmental points of view [2]. Synthesis gas is a fundamental feedstock for refining processes, such as hydrotreating and hydrocracking, for petrochemical processes, such as the synthesis of methanol, methanol to gasoline, and the synthesis of ammonia [3] and for the hydrocarbon synthesis, via Fischer–Tropsch processes [4].

Tri-reforming consists of a synergetic combination of steam reforming (Eq. (1)), dry reforming (Eq. (2)) and partial oxidation (Eq. (3)) of methane.

$$H_2O + CH_4 \rightarrow CO + 3H_2 (\Delta H^o = 206.3\,kJ\,mol^{-1}) \quad (1)$$

$$CO_2 + CH_4 \rightarrow 2CO + 2H_2 (\Delta H^o = 247.3\,kJ\,mol^{-1}) \quad (2)$$

$$CH_4 + 1/2O_2 \rightarrow CO + 2H_2 (\Delta H^o = -35.6\,kJ\,mol^{-1}) \quad (3)$$

The main advantages of this process, compared to dry and steam reforming, are the less endothermic nature of the global process (due to the presence of the exothermic methane partial oxidation reaction), the low quantity of coke generated (Eqs. (4) and (5)) due to the presence of oxidants like H_2O and O_2 (Eqs. (6) and (7)), and the possibility to modify the H_2/CO molar ratio by shifting the reactants ratio.

$$2CO \rightleftarrows C + CO_2 (\Delta H^o = -172.2\,kJ\,mol^{-1}) \quad (4)$$

* Corresponding author. Tel.: +34 926295300; fax: +34 926295256.
E-mail address: JesusManuel.Garcia@uclm.es (J.M. García-Vargas).

http://dx.doi.org/10.1016/j.apcatb.2014.09.044
0926-3373/© 2014 Elsevier B.V. All rights reserved.

$$CH_4 \rightleftarrows C + 2H_2 (\Delta H^o = 74.9\,kJ\,mol^{-1}) \quad (5)$$

$$C + H_2O \rightleftarrows CO + H_2 (\Delta H^o = 131.4\,kJ\,mol^{-1}) \quad (6)$$

$$C + O_2 \rightleftarrows CO_2 (\Delta H^o = -393.7\,kJ\,mol^{-1}) \quad (7)$$

Due to the high price and non-availability of noble metals like Pt, Rh, and Ru, transition metals have been selected as the active phase for several catalytic processes. Nickel has proven to be the most appropriate transition metal for reforming processes [5]. Moreover, nickel has been extensively studied in different reforming processes, including steam reforming [6], dry reforming [7] and partial oxidation [8].

In this work a novel support, β-Silicon carbide (β-SiC), with many interesting characteristics, was used. β-SiC exhibits a high thermal conductivity, a high resistance towards oxidation, a high mechanical strength, chemical inertness and average surface area (around 25 m^2/g) [9]. Although β-SiC-based catalysts has shown acceptable performance for methane tri-reforming [10,11], an improvement of their catalytic stability and specially their resistance against coke deactivation should be considered before considering them as potential catalysts for this process. In a previous work [12], Mg was chosen as the best promoter for Ni/β-SiC catalysts used in the tri-reforming process of methane. The presence of Mg enhanced both the activity and stability of the catalyst, leading to a decrease of the Ni metal particle size and an increase of its basicity.

In this paper, the influence of the order of Ni and Mg impregnation on the catalytic performance in the methane tri-reforming process of Ni–Mg/β-SiC catalysts was studied.

2. Experimental

2.1. Catalyst preparation

Catalysts were prepared by the wet impregnation method, using β-SiC (SICAT CATALYST) as support and nickel nitrate $Ni(NO_3)_2{\cdot}6H_2O$ (PANREAC) and magnesium hydroxide $Mg(OH)_2$ as precursors, adding the required quantity to an aqueous solution in order to obtain catalysts with a Ni load of 5 wt%. Catalysts were prepared with two different Mg/Ni molar ratios, 1/10 and 1/1. For each molar ratio, three different sets of catalysts were prepared. The first one was prepared by first Ni impregnation, followed by a calcination step (2 h at 1173 K) and subsequent Mg impregnation (samples Mg/Ni/SiC). The second one was prepared by first Mg impregnation, followed by a calcination step (2 h at 1173 K) and subsequent Ni impregnation (samples Ni/Mg/SiC). The third one was prepared by Ni and Mg co-impregnation (samples Ni–Mg/SiC). In addition, a reference catalyst prepared by just Ni impregnation was used in order to check the influence of the promoter on the performance of the methane tri-reforming process. All the catalysts were dried at 393 K overnight and calcined in air at 1173 K for 2 h.

2.2. Catalyst characterization

Ni and Mg metal loadings were determined by atomic absorption (AA) spectrophotometry, using a SPECTRA 220FS analyzer. Samples (ca. 0.5 g) were treated in 2 mL HCl, 3 mL HF and 2 mL H_2O_2 followed by microwave digestion (523 K). Surface area/porosity measurements were conducted using a QUADRASORB 3SI sorptometer apparatus with N_2 as the sorbate at 77 K. The samples were outgased at 453 K under vacuum (5×10^{-3} torr) for 12 h prior to the analysis. Specific surface areas were determined by the multi point BET method. Specific total pore volume was evaluated from N_2 uptake at a relative pressure of $P/P_o = 0.99$. Temperature-programmed reduction (TPR) experiments were conducted in a commercial Micromeritics AutoChem 2950 HP unit with TCD detection. Samples (ca. 0.15 g) were loaded into a U-shaped tube and ramped from room temperature to 1173 K (10 K min^{-1}), using a reducing gas mixture of 17.5% v/v H_2/Ar (60 cm^3 min^{-1}). CO_2 temperature-programmed desorption (TPD) experiments were conducted in a commercial Micromeritics AutoChem 2950 HP unit with TCD detection. 0.15 g of sample were loaded in a quartz tube, reduced and pretreated in He. After cooling, 30 mL min^{-1} of CO_2 (99.99% purity, Praxair certified) was passed through the sample for 30 min at a constant temperature of 323 K. Finally, the gaseous and weakly adsorbed carbon dioxide was removed by a steady flow of He for another 30 min. The sample was then heated in 50 mL min^{-1} of He with a heating rate of 10 K min^{-1} up to 1173 K. XRD analyses were conducted with a Philips X'Pert instrument using nickel-filtered Cu Kα radiation. The samples were scanned at a rate of 0.02° $step^{-1}$ over the range $5° \leq 2\theta \leq 90°$ (scan time = 2 s $step^{-1}$). Temperature-programmed oxidation (TPO) analyses were performed in a Micromeritics AutoChem 2950 HP unit, flowing 50 cm^3 min^{-1} of pure oxygen from room temperature to 1173 K (10 K min^{-1}). Transmission electron microscopy (TEM) analyses employed a JEOL JEM-4000EX unit with an accelerating voltage of 400 kV. Samples were prepared by ultrasonic dispersion in acetone with a drop of the resultant suspension evaporated onto a holey carbon-supported grid. Mean nickel particle size evaluated as the surface-area weighted diameter ($\bar{d}_s$) was computed according to Eq. (8):

$$\bar{d}_s = \frac{\sum_i n_i d_i^3}{n_i d_i^2} \quad (8)$$

where n_i represents the number of particles with diameter d_i ($\sum_i n_i \geq 400$).

2.3. Catalyst activity measurement

Experiments were carried out in a tubular quartz reactor (45 cm long and 1 cm internal diameter). The catalyst, with particle size in the range 250–500 μm and no dilution, was placed on a fritted quartz plate located at the end of the reactor. The temperature of the catalyst was measured with a K-type thermocouple (Thermocoax) placed inside the inner quartz tube. The entire reactor was placed in a furnace (Lenton) equipped with a temperature-programmed system. Reaction gases were Praxair certified standards of CH_4 (99.995% purity), CO_2 (99.999% purity), O_2 (99.99% purity), and N_2 (99.999% purity). The gas flow was controlled by a set of calibrated mass flowmeters (Brooks 5850 E and 5850 S). The water content in the reaction mixture was controlled using the vapour pressure of H_2O at the temperature of the saturator (297 K). All lines placed downstream from the saturator were heated above 373 K to prevent condensation. The saturation of the feed stream by water at the working temperature was verified by a blank experiment in which the amount of water trapped by a condenser was measured for a specific time and compared to the theoretical value. The feed composition (by volume %) was as follows: 6% CH_4, 3% CO_2, 3% H_2O, 0.6% O_2, N_2 balance, with a total flow of 100 mL min^{-1}. This composition was used in previous studies [11–14] to get a molar ratio in the feed of $CH_4/CO_2/H_2O/O_2 = 1/0.5/0.5/0.1$. In a previous work [10], it was observed that with this composition one could obtain a synthesis gas with a H_2/CO molar ratio close to the desired ratio for most of the synthesis gas applications (H_2/CO = 2). The weight hourly space velocity (WHSV) of the total gas mixture was fixed at 60,000 mL h^{-1} g^{-1}.

Prior to the reaction, the catalysts were reduced in a hydrogen pure stream at 973 K. The catalytic activity was evaluated at 1073 K and atmospheric pressures for 24 h. Gas effluents were analyzed with a micro gas chromatograph (Varian CP-4900). Methane and

Table 1
Physical properties of the catalysts.

	Ni/SiC	Mg/Ni/SiC 1/10	Ni/Mg/SiC 1/10	Ni–Mg/SiC 1/10	Mg/Ni/SiC 1/1	Ni/Mg/SiC 1/1	Ni–Mg/SiC 1/1
Ni loading (%)	4.5	4.6	4.8	5.2	4.5	4.2	5.5
Promoter loading (%)	–	0.2	0.2	0.2	1.8	1.7	1.8
Surface area ($m^2\ g^{-1}$)	23.9	22.2	21.8	22.5	21.1	16.9	21.2
Total pore volume ($cm^3\ g^{-1}$) × 10^2	14.4	10.7	11.2	13.1	13.9	11.0	12.6
Particle diameter from XRD (nm)	63	36	41	39	33	33	32
Diffraction angle of NiO (2Θ)	43.22	43.22	43.14	43.14	43.14	42.94	42.9
Particle diameter from TEM (nm)	57	–	51	–	–	32	-
Reduction degree (%)	99.8	76.9	73.3	99.4	75.3	57.8	59.0

carbon dioxide consumption rates were calculated as follows: [inlet molar flow – outlet molar flow]/nickel weight.

3. Results and discussion

3.1. Catalyst characterization

XRD results for the reduced catalysts are given in Fig. 1. In all cases the main diffraction peaks corresponding to β-SiC and Ni^0 were observed. Peaks related to the support structurally corresponded to cubic β-SiC (3C-type), their corresponding Miller indexes being indicated in Fig. 1a. Ni particle sizes (Table 1) were obtained with the Debye–Scherrer equation using data from the XRD patterns (1 1 1 reflection of Ni^0). This method has some limitations when it is used for quantitative purposes but it is useful for comparative ones. The diffraction angle of NiO for the different Mg promoted catalysts before reduction is given in Table 1. The higher the Mg content, the lower the value of this diffraction angles was. This decrease is usually attributed to the formation of a NiO–MgO solid solution [15,16], which is related to the occurrence of a great interaction between Ni and Mg. In addition, for the catalysts prepared by first Mg impregnation or by simultaneous Ni and Mg impregnation, an even lower diffraction angle was measured if compared to that of the catalysts prepared by first Ni impregnation. The formation of a solid solution between two different metals should meet the criteria determined by Hume-Rothery, which happen for Ni and Mg, as both cations have similar ionic radii, ca. 0.78 Å [17], the same common oxidation state (+2), and the same bulk oxide structure, NaCl-type [18]. This solid solution has been observed by several authors when preparing catalysts where Ni and Mg are present [19–21], and has shown high selectivity and stability in different reforming processes.

In order to check the accuracy of the XRD technique to measure the Ni metal particle size, TEM analyses were also carried out (Table 1). Some differences between the values reported by both techniques are noted although the trend is the same. The higher the load of Mg in the bimetallic catalysts, the lower the Ni particle size was. This influence of the Mg load on the Ni particle size is probably related to the formation of NiO–MgO solid solution particles, as the aggregation of Ni metal particles is depressed during the reduction process due to the presence of highly dispersed MgO [22]. Fig. 2 shows TEM images obtained for samples Ni/SiC, Ni/Mg/SiC 1/10 and Ni/Mg/SiC 1/1. Ni particles in catalysts prepared by first Mg impregnation were smaller and better dispersed.

Surface area and pore volume data (Table 1) also gave information about the catalysts. The presence of Mg led to a slight decrease of the surface area and the pore volume probably due to a partial blockage of the β-SiC pores.

Fig. 3 shows the reduction profiles obtained by the TPR technique. That of the reference catalyst, Ni/β-SiC, placed at the top of the figure, was very similar as reported elsewhere [11], showing broad peaks and two overlapped ones around 720 and 870 K, which are usually assigned to the reduction of bulk NiO. The small peak occurred at 1140 K was related to the reduction of nickel species with a higher interaction with the support, which was attributed to the formation of nickel silicate like species [23,24]. There are no clear differences in the reduction profiles of catalysts with a Mg/Ni molar ratio of 1/10. They showed two main reduction peaks (at 700–750 K and 980 K). The former was assigned to the reduction of bulk NiO whereas the later was attributed to the reduction of a NiO–MgO solid solution, phase formed during the high temperature calcinations process and also observed in the XRD results. This phase needs higher temperatures in order to be reduced due to the strong interaction between NiO and MgO. It is clearly noted that the addition of Mg, regardless impregnation order, decreased the reducibility of Ni.

On the other hand, some differences in the reduction profiles of catalysts prepared with a Mg/Ni molar ratio of 1/1 were observed. The reduction profile in catalysts prepared by first Ni impregnation kept closer to that of the previous catalysts, presenting two overlapped peaks: one with a maximum at about 720 K and another one at about 900 K. Just a reduction peak at high temperature was

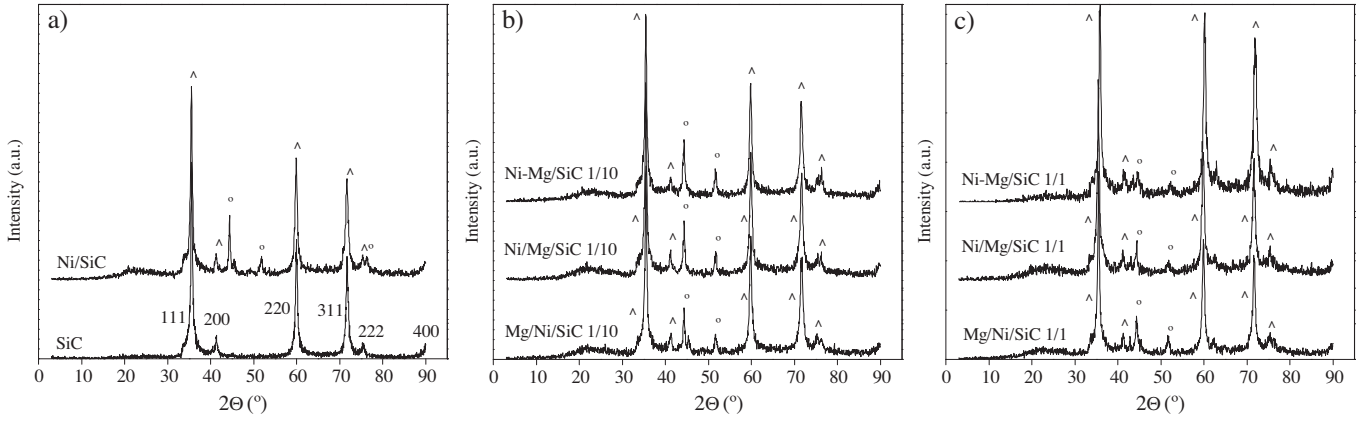

Fig. 1. XRD profiles, where (^) denotes reflection of β-SiC and (°) denotes reflection of metallic nickel.

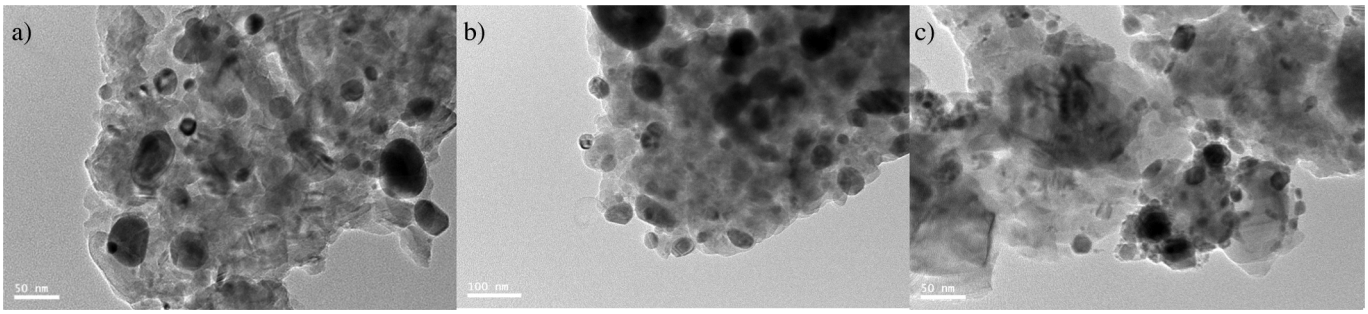

Fig. 2. TEM pictures. (a) Ni/SiC, (b) Ni/Mg/SiC 1/10, (c)Ni/Mg/SiC 1/1.

observed when Mg was firstly impregnated or when the resulting catalyst was simultaneously impregnated by Ni and Mg, which was associated to the reduction of NiO–MgO solid solution, requiring higher reduction temperatures due to the strong interaction between NiO and MgO.

It can be observed in Table 1 the reduction degree obtained from the H_2 consumption in these TPR experiments, taking into account the stoichiometry of the reduction process. Catalysts with a low Mg load showed a lower reduction degree compared to that of the reference catalysts, except for the Ni–Mg/SiC sample. This latter catalyst showed a reduction degree very close to that of the reference catalyst, despite having a profile where reduction peaks are shifted towards higher temperatures. Catalysts with a high Mg load showed even lower values of reduction degree. This is in agreement with the higher extension of the NiO–MgO solid solution, which makes the reduction process more difficult.

The desorption profiles of CO_2-TPD experiments showed a similar trend with a small desorption peak around 1100 K (Fig. 4). This desorption peak is related to adsorption points of strong basicity, as it is required a high temperature in order to desorb the CO_2 molecule. There are not significant differences in the quantity of CO_2 adsorbed for the different catalysts, as it keeps relatively low for all of them. However, as a general trend, it can be observed an increase in the quantity of CO_2 adsorbed (and therefore in the catalyst basicity) with the Mg load increase. This effect is clearer in those catalysts prepared by simultaneous impregnation of Ni and Mg.

3.2. Catalytic activity

Figs. 5 and 6 show the performance of all catalysts in the methane tri-reforming process. With the exception of catalysts prepared by first Ni impregnation, the addition of Mg improved the performance of catalysts Ni/β-SiC. Comparing the performance of catalysts with a Mg/Ni molar ratio of 1/10, it can be seen that catalysts Ni/Mg/SiC 1/10 and Ni–Mg/SiC 1/10 led to the higher methane consumption rate and presented better stability. The addition of Mg decreased the carbon dioxide consumption rate and increased the H_2/CO molar ratio, especially when Mg was firstly impregnated.

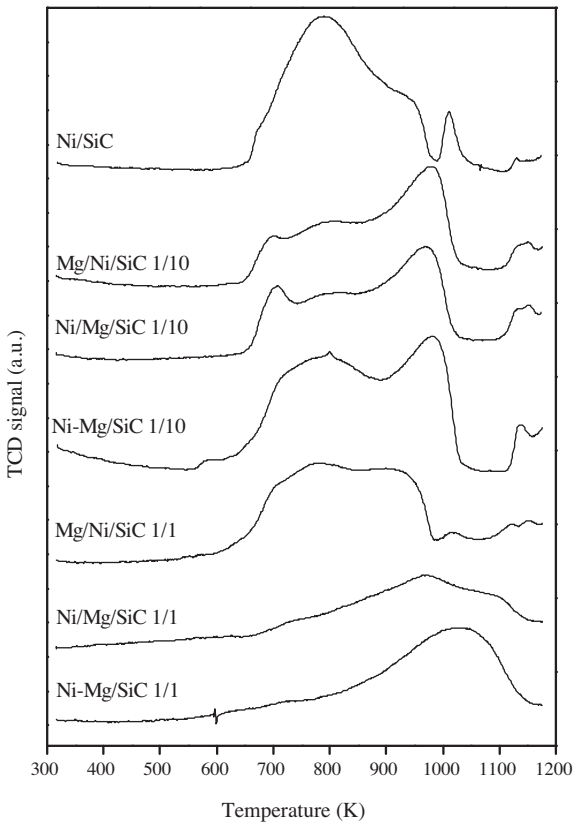

Fig. 3. Temperature programmed reduction profiles.

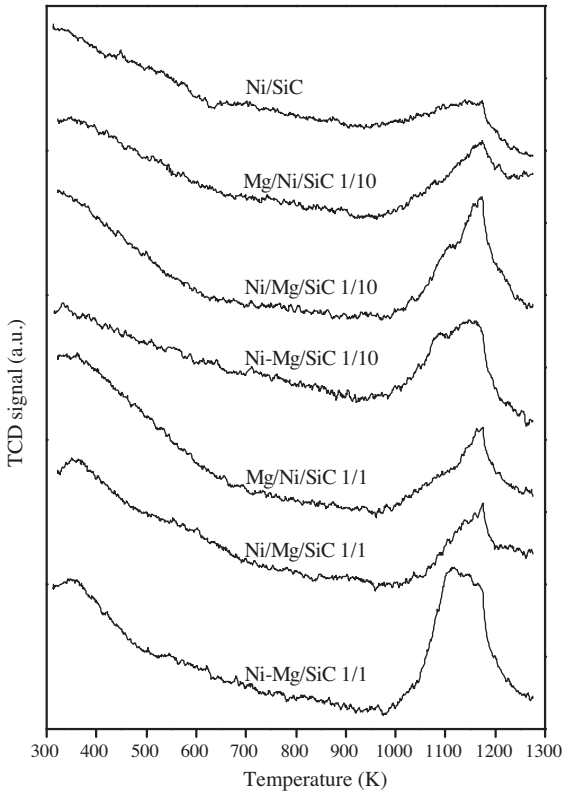

Fig. 4. CO_2 temperature programmed desorption profiles.

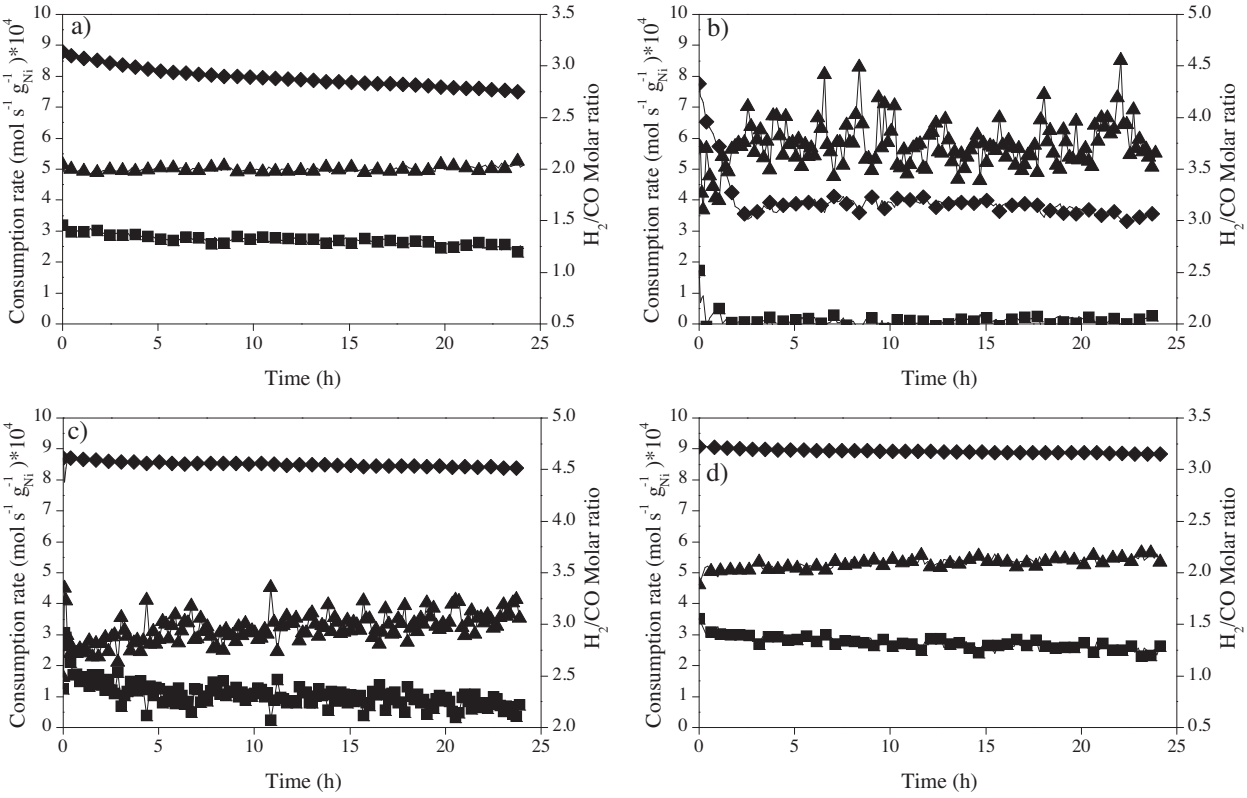

Fig. 5. Catalytic activity at 1073 K for: (a) Ni/SiC, (b) Mg/Ni/SiC 1/10, (c) Ni/Mg/SiC 1/10, (d) Ni–Mg/SiC 1/10. Reaction conditions: CH_4 = 6%, CO_2 = 3%, H_2O = 3%, O_2 = 0.6%, N_2 balance, total flow rate = 100 mL min^{-1}. CH_4 () and CO_2 () consumption rates vs. time on stream (left axis), and H_2/CO molar ratio () vs. time on stream (right axis).

This behaviour seems not to be linked with the increase in the catalyst basicity that the presence of Mg usually induces. However, as reported in a previous work [12], it could be related to both the strong basicity induced in the SiC support [25] and the higher presence of NiO species in the catalysts (as the Mg loaded catalysts are more difficult to reduce). NiO promotes the water gas shift reaction, resulting in a lower CO_2 consumption rate [26], what will increase in addition the H_2/CO molar ratio. Catalysts Ni/Mg/SiC 1/10 and Ni–Mg/SiC 1/10 presented a remarkable stability after 24 h on stream if compared to that of reference sample, demonstrating the positive influence of these preparation methods for the tri-reforming process. Catalyst Mg/Ni/SiC 1/10 showed in turn a very low catalytic activity, probably due to the blockage of the Ni active sites after Mg impregnation.

Table 2 lists the main reaction parameters obtained with all the catalysts. The reference catalyst showed a good methane consumption rate but a remarkable deactivation after 24 h of time on stream. The addition of Mg as promoter after Ni impregnation led to a decrease of both the methane consumption rate and the catalyst stability. This behaviour seems to be related to the predominant interaction of the Ni particles with the support, rather than with the promoter [27], as well as to the more difficult access of the reaction gases to the Ni metal particles. In addition, the H_2/CO molar ratio obtained was very high while the CO_2 consumption rate was kept very low, demonstrating that dry reforming did not greatly contribute to the global tri-reforming process. Methane consumption rate values and catalytic stability for catalysts Ni/Mg/SiC and Ni–Mg/SiC with a Mg/Ni molar ratio of 1/10 resembled very similar, showing a catalytic activity slightly higher than that obtained for the reference catalyst. The presence of Mg in these catalysts had a positive effect, which was related to the above mentioned interaction between Ni and Mg. In addition, this interaction allowed both the presence of smaller Ni particles, favouring a higher reforming activity and a smaller coke rate deposition [28,29], and the simultaneous formation of a Ni–Mg solid solution, confirmed by the XRD results and the TPR experiments, leading to Ni to strongly interact with Mg, which in turn also hindered coke formation [30,31].

Fig. 6 shows the performance of catalysts with a Mg/Ni molar ratio of 1/1. Very high and stable catalytic activity was obtained for samples Ni/Mg/SiC and Ni–Mg/SiC, being the values of methane consumption rate around 9×10^{-4} mol s^{-1} g$_{Ni}^{-1}$. Similar values were obtained for catalysts with a Mg/Ni molar ratio of 1/10 but, H_2/CO molar ratio in the downstream was slightly higher. Again, the catalyst prepared by first Ni impregnation showed the poorest catalytic behaviour, with very low methane and carbon dioxide consumption rates and a worse stability with the time on stream.

Table 2 also lists the main reaction parameters obtained with all the catalysts. Catalyst Mg/Ni/SiC 1/1 showed the worst catalytic results at all, including those of the reference catalyst. As previously commented, the impregnation of Mg after Ni made the latter to weakly interact with the former and hinder methane access to the active sites. As was confirmed by XRD, the higher the amount of Mg, the stronger the interaction of both metals was. This higher interaction seemed to improve the catalytic activity but did not balance the negative effect of Ni particles blockage. Methane consumption rates for catalysts Ni/Mg/SiC and Ni–Mg/SiC with a Mg/Ni molar ratio of 1/1 resembled those obtained for catalysts prepared with a Mg/Ni molar ratio of 1/10. However, the formers presented a better catalytic performance due to the beneficial effect of Mg on the catalyst stability, due to a lower coke formation rate, as it will be discussed in the next section.

Reduction degree (Table 1) does not seem to have a clear effect on the catalytic behaviour of the catalysts reported in this work. For instance, it can be observed that Mg/Ni/SiC 1/10 and Ni/Mg/SiC 1/10 yielded very different reaction rates, despite having a similar reduction degree. In addition, catalysts with a Ni/Mg molar ratio

Table 2
Reaction and characterization after reaction parameters.

	Ni/SiC	Mg/Ni/SiC 1/10	Ni/Mg/SiC 1/10	Ni–Mg/SiC 1/10	Mg/Ni/SiC 1/1	Ni/Mg/SiC 1/1	Ni–Mg/SiC 1/1
Average CH_4 reaction rate $(mol\ s^{-1}\ g_{Ni}^{-1}) \times 10^4$	7.96	3.99	8.50	8.92	5.28	8.77	8.65
Drop in CH_4 reaction rate after 24 h of time on stream $(mol\ s^{-1}\ g_{Ni}^{-1}) \times 10^4$	1.30	4.34	0.30	0.24	1.27	0.00	0.08
Average CO_2 reaction rate $(mol\ s^{-1}\ g_{Ni}^{-1}) \times 10^4$	2.72	0.12	1.05	2.72	0.25	1.48	1.84
Drop in CO_2 reaction rate after 24 h of time on stream $(mol\ s^{-1}\ g_{Ni}^{-1}) \times 10^4$	0.76	1.55	0.51	0.45	0.35	2.56	0.74
Average H_2/CO molar ratio	2.00	3.73	2.96	2.09	3.36	2.79	2.76
Oxygen consumption in TPO ($\mu mol\ g^{-1}$)	35.28	23.44	4.04	10.70	10.81	3.72	6.24

of 1/1 showed a lower reduction degree, leading to less Ni^0 species available, but their catalytic performance was not halted. However, the different interactions between support, Ni and Mg, depending on the impregnation order, have a very important effect on the catalytic behaviour of the catalysts, even affecting to the oxidation state of the catalysts after reaction, as will be discussed in the next section.

3.3. Characterization after reaction

Temperature programmed oxidation was performed on the aged catalysts in order to quantify the coke generated during the tri-reforming process (Fig. 7). As observed, the addition of Mg avoided the formation of coke, especially for the catalysts prepared with a Ni/Mg molar ratio of 1/1 as a probable consequence of their lower Ni particle size and higher interaction between Ni and Mg. The total amount of oxygen consumed in the TPO experiments is shown in Table 2. Aged catalysts with the lower coke content were those prepared by first Mg impregnation. They were followed by those

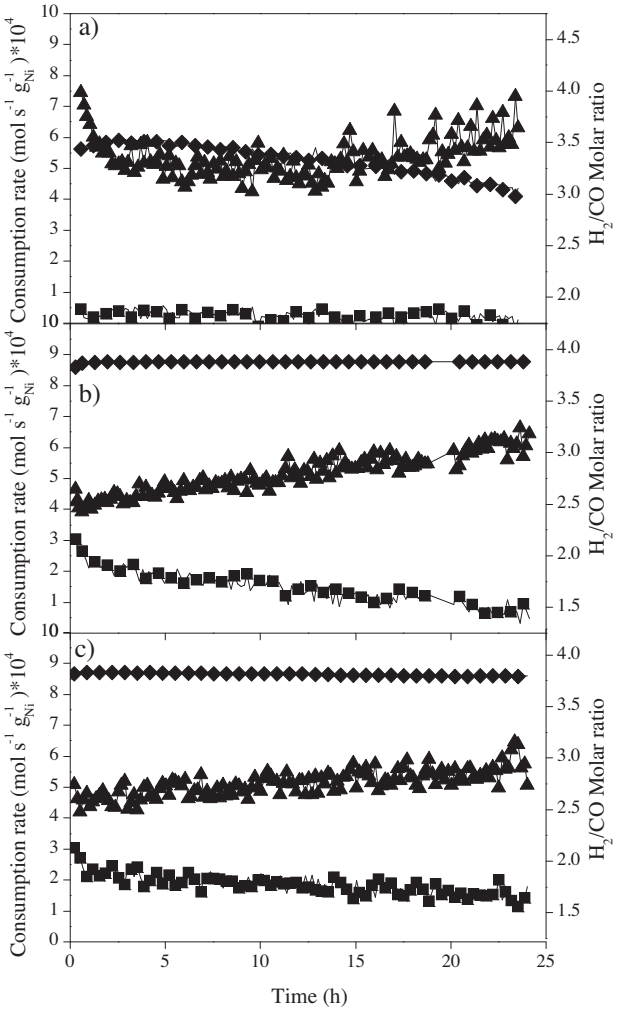

Fig. 6. Catalytic activity at 1073 K for: (a) Mg/Ni/SiC 1/1, (b) Ni/Mg/SiC 1/1, (c) Ni–Mg/SiC 1/1. Reaction conditions: CH_4 = 6%, CO_2 = 3%, H_2O = 3%, O_2 = 0.6%, N_2 balance, total flow rate = 100 mL min^{-1}. CH_4 () and CO_2 () consumption rates vs. time on stream (left axis), and H_2/CO molar ratio () vs. time on stream (right axis).

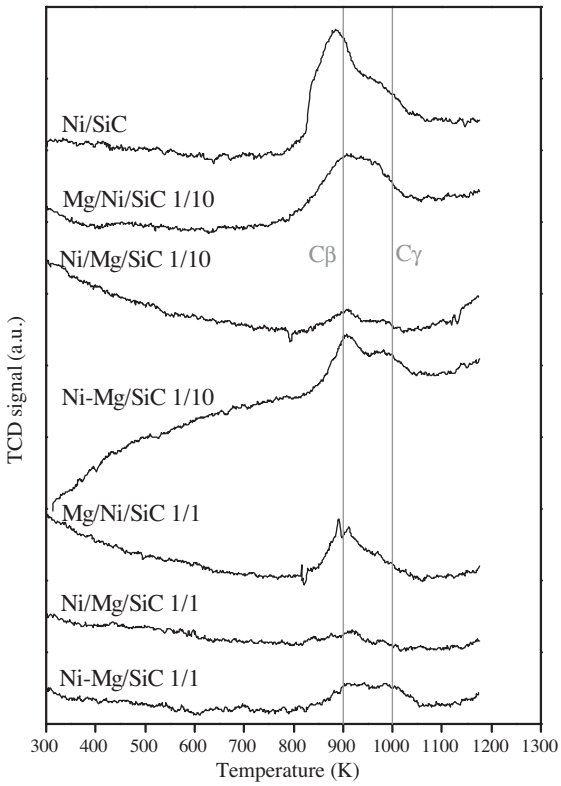

Fig. 7. Temperature programmed oxidation profiles after reaction.

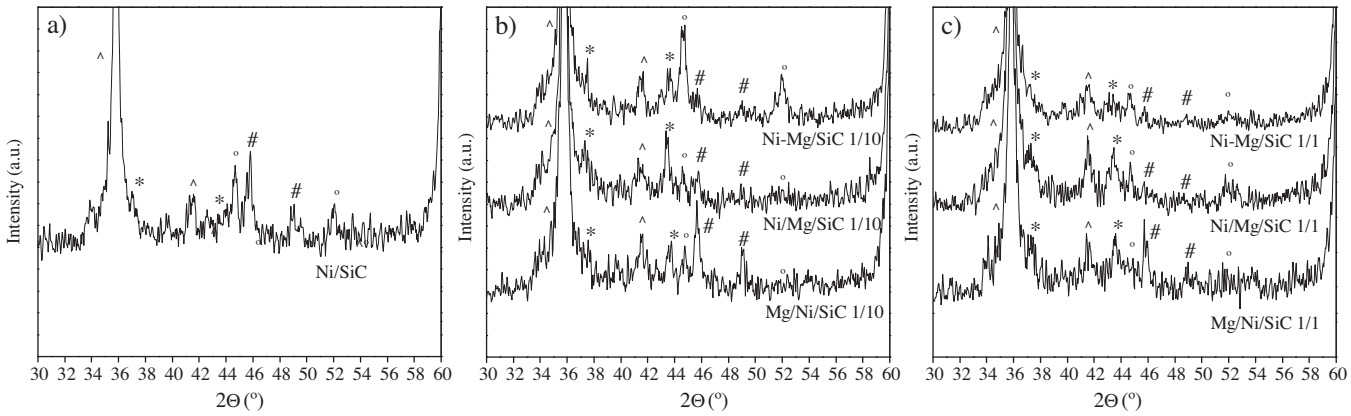

Fig. 8. XRD profiles, where (^) denotes reflection of β-SiC, (°) denotes reflection of metallic nickel, (*) denotes reflection of nickel oxide and (#) denotes reflection of Ni_2Si.

prepared by simultaneous impregnation. Two peaks with maxima around 900 and 1000 K, which would correspond to the occurrence of the C_β and C_γ coke species reported by Zhang et al. [32], are observed in Fig. 7. The former would be related to the generation of CO at high reaction temperatures whereas the latter would be responsible of the catalyst deactivation. Our results show that the addition of Mg decreases the formation of both coke species, leading to an increase of the catalyst stability.

Fig. 8 reports the X-ray diffraction patterns obtained for the aged catalysts. The reference sample (Fig. 8a) showed two peaks at 45.50° and 48.76°, which can be ascribed to the orthorhombic phase of Ni_2Si [33]. This compound was also present on the surface of aged catalysts Mg/Ni/SiC 1/10 and Mg/Ni/SiC 1/1, as observed in Fig. 8b and 8c, respectively, where the corresponding peaks appeared sharp and well defined at the same 2Θ values. This phase, which is stable up to 950 °C, is a consequence of the direct reaction between metallic Ni and SiC that is thermally activated over 600 °C [34]. In other catalysts, these peaks are smaller or do not exist, indicating that the simultaneous or previous Mg impregnation decreases the interaction between Ni and Si. According to the results listed in Table 2, the formation of Ni_2Si (leading to a lesser availability of Ni active sites) seems to be related to lower methane reaction rates and a higher extension of the deactivation processes. Diffraction peaks assigned to NiO also appeared in aged catalysts, although they are less evident in catalysts Ni–Mg/SiC 1/10 and Ni–Mg/SiC 1/1. These catalysts led to a higher average CO_2 reaction rate if compared to that of catalysts Ni/Mg/SiC 1/10 and Ni/Mg/SiC 1/1. Consequently, it could be concluded that the presence of NiO species in the latter catalysts should promote the water gas-shift reaction.

The data obtained from the XRD patterns after reaction clearly point the key importance of the impregnation order in the catalytic behaviour of the prepared catalysts. In this sense, a great attention should be paid to the processes that take place in the catalysts, not only during the high temperature calcination, but also during the tri-reforming process. The high temperature needed for this reaction and the presence of oxidants in the reaction media make possible different reactions that can be harmful for the catalytic activity. Ni can react with the β-SiC support yielding different Ni silicide compounds, or it can be oxidized by the oxygen or water fed to the system. From the data obtained, it seems to be that Mg impregnation affect both processes, and can avoid the formation of these compounds. Hence, a proper interaction between Ni and Mg improves the catalytic behaviour for the tri-reforming process.

4. Conclusions

The addition of Mg to a Ni/β-SiC catalyst, whenever it is not loaded after Ni impregnation, promoted the catalytic behaviour of the methane tri-reforming process. Catalysts where Ni was firstly impregnated showed the worst catalytic behaviours, probably due to a poor interaction between Ni and Mg, a possible blockage of the Ni particles by Mg and the formation of Ni_2Si, which decreased the number of Ni active sites. Catalysts prepared with a higher Mg/Ni molar ratio (1/1) showed smaller Ni particle sizes, a lower coke rate formation, a higher basicity and a higher Ni-Mg interaction. Catalysts where Mg was firstly impregnated were less deactivated keeping a good catalytic behaviour. Simultaneous impregnation of Ni and Mg yielded catalysts with the best catalytic performances, which was related to the high interaction between Ni and Mg due to the formation of a Ni-Mg solid solution. Catalyst Ni–Mg/SiC 1/1 was selected as the best one due to its high catalytic activity, great stability and low coke production.

Acknowledgements

The authors would like to thank the Program INNOCAMPUS of the University of Castilla-La Mancha (PEID 5-3), the Consejería de Ciencia y Tecnología of the Junta de Comunidades de Castilla-La Mancha (Project PPII10-0045-5875) and the Spanish government (grant FPU AP2009-2948) for their financial support.

References

[1] U.S.D.o.E.O.o. Science, U.S.O.o.F Energy, Carbon Sequestration: State of the Science: A Working Paper for Roadmapping Future Carbon Sequestration R&D, 1999.
[2] J. Xu, W. Zhou, Z. Li, J. Wang, J. Ma, Int. J. Hydrogen Energy 34 (2009) 6646–6654.
[3] M.A. Peña, J.P. Gómez, J.L.G. Fierro, Appl. Catal. A: Gen. 144 (1996) 7–57.
[4] H.-t. Jiang, H.-q. Li, Y. Zhang, J. Fuel Chem. Technol. 35 (2007) 72–78.
[5] J.S. Kang, D.H. Kim, S.D. Lee, S.I. Hong, D.J. Moon, Appl. Catal. A: Gen. 332 (2007) 153–158.
[6] D.H. Prasad, H.I. Ji, H.R. Kim, J.W. Son, B.K. Kim, H.W. Lee, J.H. Lee, Appl. Catal. B: Environ. 101 (2011) 531–539.
[7] A. Kambolis, H. Matralis, A. Trovarelli, C. Papadopoulou, Appl. Catal. A: Gen. 377 (2010) 16–26.
[8] H. Özdemir, M.A. Faruk Öksüzömer, M. Ali Gürkaynak, Int. J. Hydrogen Energy 35 (2010) 12147–12160.
[9] D.L. Nguyen, P. Leroi, M.J. Ledoux, C. Pham-Huu, Catal. Today 141 (2009) 393–396.
[10] J.M. García-Vargas, J.L. Valverde, A. de Lucas-Consuegra, B. Gómez-Monedero, F. Dorado, P. Sánchez, Int. J. Hydrogen Energy 38 (2013) 4524–4532.
[11] J.M. García-Vargas, J.L. Valverde, A. De Lucas-Consuegra, B. Gómez-Monedero, P. Sánchez, F. Dorado, Appl. Catal. A: Gen. 431–432 (2012) 49–56.
[12] J.M. García-Vargas, J.L. Valverde, J. Díez, P. Sánchez, F. Dorado, Appl. Catal. B: Environ. 148–149 (2014) 322–329.
[13] C. Song, W. Pan, Catal. Today 98 (2004) 463–484.
[14] C. Song, Chem. Innov. 31 (2001) 21–26.
[15] Y.-H. Wang, H.-M. Liu, B.-Q. Xu, J. Mol. Catal. A: Chem. 299 (2009) 44–52.
[16] F. Arena, F. Frusteri, A. Parmaliana, L. Plyasova, A.N. Shmakov, J. Chem. Soc., Faraday Trans. 92 (1996) 469–471.
[17] R.A.T.P.K. Flinn, Engineering Materials and Their Applications, Wiley, New York; Chichester, 1995.

[18] V.E.C.P.A. Henrich, The Surface Science of Metal Oxides, Cambridge University Press, Cambridge; New York, 1994.
[19] Y. Hu, E. Ruckenstein, Catal. Lett. 36 (1996) 145–149.
[20] K. Tomishige, Y. Himeno, Y. Matsuo, Y. Yoshinaga, K. Fujimoto, Ind. Eng. Chem. Res. 39 (2000) 1891–1897.
[21] Y.H. Hu, Catal. Today 148 (2009) 206–211.
[22] T. Nakayama, N. Ichikuni, S. Sato, F. Nozaki, Appl. Catal. A: Gen. 158 (1997) 185–199.
[23] Y.P. Tulenin, M.Y. Sinev, V.V. Savkin, V.N. Korchak, Catal. Today 91–92 (2004) 155–159.
[24] B. Mile, D. Stirling, M.A. Zammitt, A. Lovell, M. Webb, J. Catal. 114 (1988) 217–229.
[25] L. Pino, A. Vita, F. Cipitì, M. Laganà, V. Recupero, Appl. Catal. B: Environ. 104 (2011) 64–73.
[26] S.H. Kim, S.-W. Nam, T.-H. Lim, H.-I. Lee, Appl. Catal. B: Environ. 81 (2008) 97–104.
[27] Z. Cheng, Q. Wu, J. Li, Q. Zhu, Catal. Today 30 (1996) 147–155.
[28] D.L. Trimm, Catal. Today 49 (1999) 3–10.
[29] V.C.H. Kroll, H.M. Swaan, C. Mirodatos, J. Catal. 161 (1996) 409–422.
[30] M. Kong, J. Fei, S. Wang, W. Lu, X. Zheng, Bioresour. Technol. 102 (2011) 2004–2008.
[31] K.O. Christensen, D. Chen, R. Lødeng, A. Holmen, Appl. Catal. A: Gen. 314 (2006) 9–22.
[32] Z.L. Zhang, X.E. Verykios, Catal. Today 21 (1994) 589–595.
[33] X. Chen, A. Zhao, Z. Shao, C. Li, C.T. Williams, C. Liang, J. Phys. Chem. C 114 (2010) 16525–16533.
[34] F. Basile, P.D. Gallo, G. Fornasaria, D. Gary, V. Rosetti, A. Vaccari, Stud. Surf. Sci. Catal. 167 (2007) 313–318.